ANALYSIS OF THE THERMAL IGNITION AND INDUCTION TIME OF PREMIXED ETHANOL AND AIR COMBUSTION

Leonel Rincón Cancino
Laboratório de Combustão e Engenharia de Sistemas Térmicos. – labCET
Universidade Federal de Santa Catarina.
Campus Universitário, Trindade
CEP 88040-900, Florinaópolis, SC, Brazil.
leonel@cet.ufsc.br

Amir Antônio Martins Oliveira
Laboratório de Combustão e Engenharia de Sistemas Térmicos. – labCET
Universidade Federal de Santa Catarina
Campus Universitário, Trindade
CEP 88040-900, Florinaópolis, SC, Brazil
amirol@emc.ufsc.br

Abstract. Here we analyze the thermal ignition of ethanol (C_2H_5OH) and dry standard air using a zero-dimensional model with detailed chemistry. The variation with time of the species concentrations and the induction period for the thermal ignition process are analyzed as a function of the pressure and mixture stoichiometric ratio. The Marinov and the Konnov detailed chemical kinetic mechanisms are used in CANTERA and CHEMKIN for the simulations of ignition in constant pressure, adiabatic, perfectly stirred reactor conditions. Computational chemistry methods are used to complement the thermodynamic database and to obtain other molecular structural information. It is observed that the induction period for the thermal ignition decreases with the increase of pressure and increases with the increase of stoichiometric ratio and that the variation of induction time becomes smaller as the pressure increases. This is the same behavior as observed for the thermal ignition of aliphatic non-saturated hydrocarbons.

Keywords: Combustion, chemical kinetics, spark ignition engines, ethanol.

1. Introduction

Currently, ethanol (C_2H_5OH) and methyl tert-butyl ether (MTBE $C_4H_9OCH_3$) are the most widely employed oxygenated fuels in the transportation sector, used both as an additive and as a neat fuel. Since the elimination of tetra-ethyl lead as a gasoline additive in the mid-1980s, ethanol and MTBE have been used as an octane number enhancer and oxygen source to reduce carbon monoxide emissions. Ethanol can be synthesized from biomass, a renewable energy source, while MTBE is obtained from isobutene, which in turn is obtained from the refining of gasoline. Methanol is another oxygenated fuel also obtained from the refining of oil. Therefore, since ethanol can be obtained from biomass, it presents advantages for the carbon dioxide atmospheric balance. Ethanol has also advantages from the human health point of view since MTBE is pointed as being possibly a carcinogen substance (Marinov, 1998) and methanol is more toxic than ethanol.

The chemical kinetics of the combustion of ethanol is more complex than the kinetics of methanol (Gardiner, 2000). While methanol has been better studied, both experimentally and theoretically, e.g., Warnatz (1999) analyzed the spark ignition of methanol using a 2D-LIF (Laser Induced Fluorescence) system; few studies have been devoted to the homogeneous combustion of ethanol (Glassman, 1996; Marinov, 1998; Lin, 2002; and Gardiner 2000), each with a specific focus.

Glassman (1996) analyzed the oxidation of oxygenated hydrocarbons and explained that since the *C-C* bond is weaker than the *C-OH* bond (by 5 kcal/mol; Marinov, 1998), the thermal decomposition initiates with the methyl group abstraction, instead of the hydroxyl group abstraction. Lin (2002) analyzed the unimolecular decomposition of ethanol using an *ab-initio* method and a RRKM (Rice-Ramsperger-Kassel-Marcus) model for the prediction of the velocity constants and branching ratios. He found that the thermal decomposition of ethanol is strongly pressure and temperature dependent. Gardiner (2000) analyzed numerically the thermal ignition of ethanol using the GRIMech 1.2 mechanism completed with reactions from the mechanism reported by Chevalier (1992) (Gardiner (2000) *apude* Chevalier (1992)). He observed that all intermediate species are rapidly converted to CO_2 and H_2O right after ignition. He studied mixtures of 3% (volume) of ethanol in air at the initial temperature 1300 K. Catalytic reactions with ethanol have also been studied. Kamalkumar (2001) analyzed the catalytic reaction of ethanol, acetic acid e ethyl acetate over silica supported platinum, using DFT (Density Functional Theory) to describe the various states of the absorbed species and platinum transitions.

Marinov (1998) developed a detailed kinetic mechanism for the high-temperature oxidation of ethanol. The detailed kinetics was built by assembling previous mechanisms for hydrogen, methane, ethylene, ethane and propane oxidation. The scheme relied on literature based kinetic data, evaluated kinetic rate constant information, theoretically calculated

rate parameters and rate constant and relied also on estimations based on analogies to similar systems. The main ethanol oxidation routes developed are shown in Figure 1. These oxidation routes lead ultimately to the production of methane, formaldehyde and other oxygenated hydrocarbons, whose kinetics are well treated by other detailed mechanisms (methane, etc.). The high temperature ethanol oxidation occurs by two main routes. One route occurs by decomposition triggered by a third body collision. The decomposition reactions are:

$$C_2H_5OH\left(+M\right) \rightleftarrows CH_3 + CH_2OH\left(+M\right)$$
$$C_2H_5OH\left(+M\right) \rightleftarrows C_2H_4 + H_2O\left(+M\right)$$
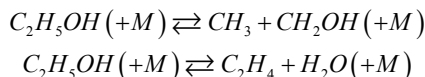
While the C_2H_4 route consumes most of the ethanol (in mass), the CH_3 route parameters present a higher sensitivity in calculated ignition delay times and must be determined with more care. Computational chemistry tools where used to obtain the kinetic parameters of the decomposition reactions.

The other route occurs by hydrogen abstraction by a radical collision. There are three possible positions for the hydrogen to be removed. One is the hydrogen bond to the CH_3 group, named a primary hydrogen, or Hp. The second is the hydrogen bond to the CH_2OH group, named a secondary hydrogen, or Hs. The third is the hydrogen bond to the OH group, named the hydroxyl hydrogen, or Hx. These possible paths are represented as:

$$C_2H_5OH + X \rightarrow CH_2CH_2OH + XH$$
$$C_2H_5OH + X \rightarrow CH_3CHOH + XH$$
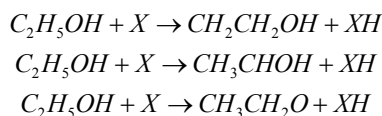$$C_2H_5OH + X \rightarrow CH_3CH_2O + XH$$

Table 2 presents the bond lengths and bond energies for the ethanol molecule. The main concern in developing the mechanism was to properly obtain the branching ratio for the *H*-atom abstraction for the different channels, and the T dependence of the branching ratio. The branching ratio assignment was developed based on the kinetics for other species that exhibit similar bond strengths and structural characteristics, such as methanol, which presents Hs and Hp bonds, and propane, which presents Hs and Hx bonds. Some of the findings reveal that the hydrogen abstraction occurs through collisions with mainly four radicals, OH, O, H and CH_3. The *H*-atom abstraction with OH is the primary role for OH in the ethanol oxidation. It is observed experimentally that the OH termination reaction $OH + HO_2 \rightarrow H_2O + O_2$ slows down the ethanol oxidation.

The kinetic mechanism was compared to measurements available from the literature for the stoichiometric ratio from 0.5 to 2, initial temperatures from 1000 to 1700 K and pressures from 1.0 to 4.5 atm. Experimental results were available for ignition delay from shock tubes, laminar flame speed in burners, and product distribution from pyrolysis and oxidation studies in static, turbulent flow and jet-stirred reactors. Other observations from static and flow reactors, autoignition behavior in rapid compression machines and combustion bomb, and formation of soot in diffusion flames have been useful in developing the mechanism. Table 1 presents an overview of the chemical mechanism.
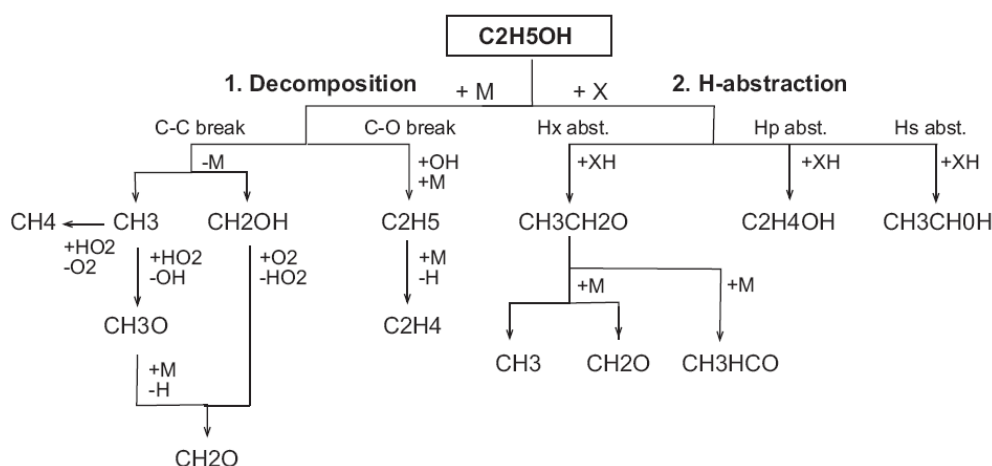

Figure 1. Main ethanol high-temperature oxidation routes (adapted from Marinov, 1998).

The mechanism by Konnov (2000) was developed for the combustion of hydrocarbons with at most three carbon atoms in the molecule. This mechanism has been compared to other mechanisms in the literature for the combustion of methane, propane, butane and acetylene (Cancino, 2004; Cancino and Oliveira, 2004, 2005) and a good comparison was obtained. This mechanism has not been used in the literature for predicting the combustion of ethanol. Nevertheless,

Konnov (2005) mentions that it might be basically able to predict the combustion of ethanol when the additional thermodynamic properties are given. We note that, the ethanol decomposition and *H*-atom abstraction leads ultimately to C_2 hydrocarbons and oxygenated species, whose kinetics are included into the comprehensive Konnov mechanism. Table 1 presents an overview of this chemical mechanism.

Here, we analyze numerically the thermal ignition of ethanol with dry standard air using the two kinetic mechanisms available from the literature, the Marinov and the Konnov mechanisms. The Marinov mechanism is understood as a base mechanism validated with literature measurements. Our objective is two-fold: first, it is to map the variation of the ignition delay time for constant pressure combustion of ethanol with dry air as a function of pressure and stoichiometric ratio, using the Marinov mechanism. Second, it is to compare the results obtained from the Konnov mechanism in order to access its potential to predict the ethanol combustion. This second objective is aimed to the overall idea of developing a single reduced chemical mechanism able to model the kinetics of ethanol and hydrocarbon mixtures and as a basis for the development of kinetic mechanism for heavier hydrocarbons (up to C_8).

Table 1. Overview of two chemical kinetic mechanisms for the combustion of ethanol with dry standard air.

Mechanism	Elements	Chemical Species	Elementar Reactions	NOx Kinetics	Pressure Range (atm)
Marinov	4	57	383	No	1.0 - 4.5
Konnov	5	127	1200	Yes	0.0921 - 7.5

The results here will be presented as a function of the fuel stoichiometric ratio defined in molar basis as

$$\Phi = \frac{\left(Air / Fuel \right)}{\left(Air / Fuel \right)_{St.}} \tag{1}$$

where (*Air/Fuel*) is the actual air-fuel molar ratio and (*Air/Fuel*)$_{St.}$ is the stoichiometric air-fuel molar ratio.

For all computation, the initial temperature of the mixture is 1200 K.

2. Molecular structure data and thermodynamic properties of ethanol

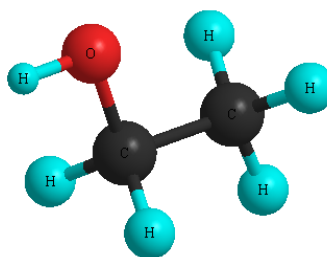Figure 2 presents a standard representation of the molecular structure of ethanol.

Figure 2. Molecular structure of ethanol.

Table 2 presents the values of the thermodynamic properties of ethanol obtained from computational chemistry simulations using the software GAMESS (*General Atomic and Molecular Electronic Structure System*) from Iowa State University, using a functional basis HF/6-31G(d,p). The functional basis is a set of mathematical functions from which the wave function is built (Cramer, 2002). We note that the results obtained from computational chemistry depend strongly on the functional basis used. Here we chose to use the basis HF/6-31G(d,p), i.e., a basis that uses a Hartree-Fock method with 6 primitive gaussian functions (HF/6) and one double zeta function (31) completed with a *d* function for the heavy atoms and a *p* function for the hydrogen atoms. The entropy and enthalpy of formation values agree well with the values listed from the JANNAF table.

From Table 2 we note also the different bong strengths for the *C-H*, *C-C* and *C-O* bonds. The *C-Hs* bond has a strength of 96-98 kcal/mol, the *C-Hp* has a strength of 98-100 kcal/mol and the *O-Hx* bond has a strength of 104 kcal/mol. The bonds break following different kinetic parameters. The sum of the three kinetics must reproduce the overall kinetics for *H*-atom abstraction from ethanol. This was adjusted by Marinov (1998).

The values listed for the *C-C* and *C-O* bond strengths listed in Table 2 where obtained from Kuo (1986). Marinov (1998) cites that the *C-C* bond is about 5 kcal/mol weaker than the *C-O* bond.

Table 2. Thermodynamic and molecular structural properties for ethanol.

		Bond Lenght [Angstrom]		Bond Energy [kJ/mol]		Thermodynamic Properties @ 298,15 K		Basis set
						Cp J/(mol K)	S J/(mol K)	
C_2H_5OH	Group COH	$C-O$	(1.4037)	360	(1)			
		$C-H$	(1.0896)	402-410	(2)			
		$O-H$	(0.9424)	435	(1)			
	Group CH_3	$C-H$	(1.0858)	410-419	(2)	61,5	267,23	HF / 6-31G(d,p)
		$C-H$	(1.0844)					
		$C-H$	(1.0844)					
	Group C_2	$C-C$	(1.5151)	358	(2)			

(1) Kuo, 1986, (2) Marinov, 1998

3. Thermal ignition

CANTERA (2001) and CHEMKIN (2003) were used to simulate the thermal ignition of ethanol in constant pressure, adiabatic, perfectly stirred reactor conditions. The induction period, and the time evolution of temperature and mole fractions of intermediate species were observed as a function of pressure and stoichiometric ratio.

From the literature (e.g., Warnatz, 1999), the ignition point is assigned to the destruction of fuel, formation of carbon monoxide, formation of hydroxyl radical, a given pressure increment in a constant volume process, a given temperature increment in a constant pressure process, etc.. These choices are mainly related to the physical process or experiment that someone is interested in analyzing or comparing the numerical predictions. Here, the point of inflection of the temperature versus time curve is used as the ignition point. This point also coincides with the maximum heat release point and also roughly scales to the point with 400 K heating above the initial temperature, used by CANTERA (2001) and CHEMKIN (2003). The induction period is the time elapsed since the beginning of the chemical reactions and the ignition point.

The time evolution of the temperature as a function of stoichiometric ratio for a total pressure of 1 atm predicted by the Marinov (1998) mechanism is shown in Figure 3.
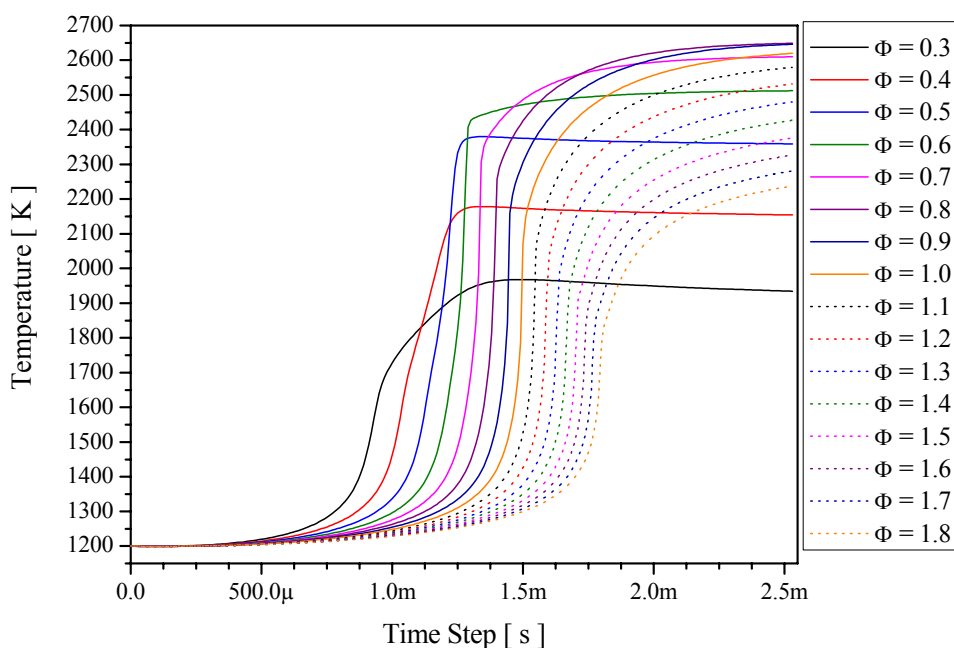

Figure 3. Time evolution of the temperature as a function of stoichiometric ratio for a total pressure of 1 atm predicted by the Marinov (1998) mechanism (obtained with CANTERA).

From Figure 3 we note that the induction period increases as the initial mixture becomes lean in fuel (the amount of air in the initial mixture increases). This behavior is the same detected for the unsaturated aliphatic hydrocarbons (Cancino, 2004; Cancino and Oliveira, 2005). The results obtained from the Konnov (2000) mechanism show the same general trend, however, with a stronger dependency on the total pressure of the system. Figure 4 presents the time variation of the system temperature as predicted by the Marinov and the Konnov mechanisms for stoichiometric conditions for two different values of pressure.
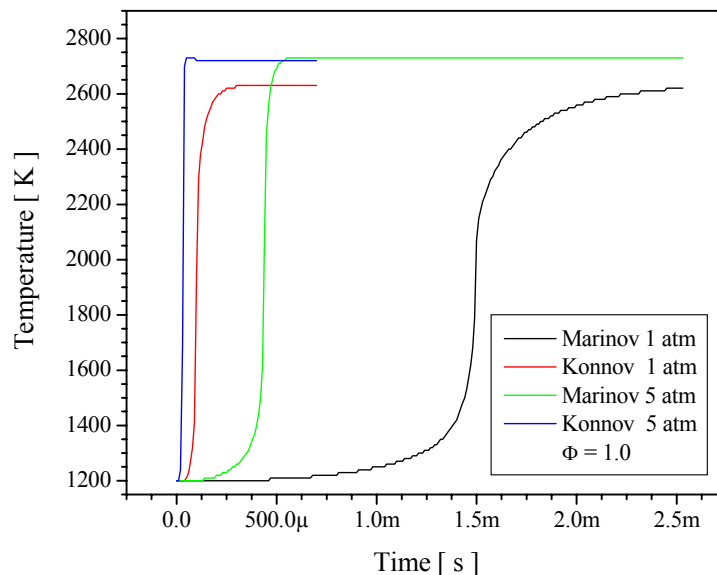

Figure 4. Time evolution of temperature as predicted by the Marinov and Konnov mechanisms for stoichiometric mixture and two values of total pressure (obtained with CHEMKIN).

It can be observed that both mechanisms result in the same final temperature for the same initial pressure. This can be considered as a partial validation of the Konnov mechanism, since this implies that the thermodynamic properties used are consistent. Also, since the temperature evolves in a similar way, it implies that the main reaction mechanisms and equilibrium constants are being calculated consistently. It is not a simple task to compare directly the formation of intermediate products since each mechanism deals with a different total number of chemical species (Table 1). We note also that the Marinov mechanism predicts a longer induction period and the difference increases for the lower pressure. This indicates a failure in the Konnov mechanism in correctly predicting the formation and destruction of intermediate species. Since the mechanism by Marinov has been validated in the pressure range from 1 to 5 atm, it will be used in the subsequent results.

In figure 4, we note that the induction period decreases with the increase in the total pressure of the system. Figure 5 presents the time variation of the system temperature as predicted by the Marinov mechanism for stoichiometric conditions for values of pressure increasing from 1 to 5 atm. It can be seen that the time evolution of temperature becomes steeper and the induction period decreases with the increase in pressure. We note a small effect of the total pressure in the final temperature of the system. The increase of final temperature as a consequence of the increase in total pressure is typical of exothermic reactions (Glassman, 1996).

The variation of induction period with pressure is better analyzed in figure 6. Figure 6 presents the variation of the induction period with the stoichiometric ratio for different values of pressure as predicted by the Marinov (1998) mechanism. It can be observed that the induction period decreases as the pressure is increased and the variation with the stoichiometric ratio is smaller for the higher pressures, ranging from 1000 to 1800 µs at 1 atm and 200 to 500 µs at 5 atm. It can be observed also a change of regime for stoichiometric ratio around 0.5. The rate of change of the induction period with the stoichiometric ratio is the same for pressures between 3 to 5 atm. We can attempt to explain the dependence of the induction period in the pressure from an analysis of the formation and destruction of intermediate species.

Figure 7 shows the time variation of the mole fractions of the major intermediate species (OH, CH_3, HO_2, CO) and the saturated combustion products (CO_2, H_2O). We note that the variation in pressure does not have an important effect on the maximum amount of OH produced. The time variation of the mole fraction follows the same trends exhibited by the temperature, but it is interesting to note that the destruction of OH is progressively slower as the pressure is reduced.
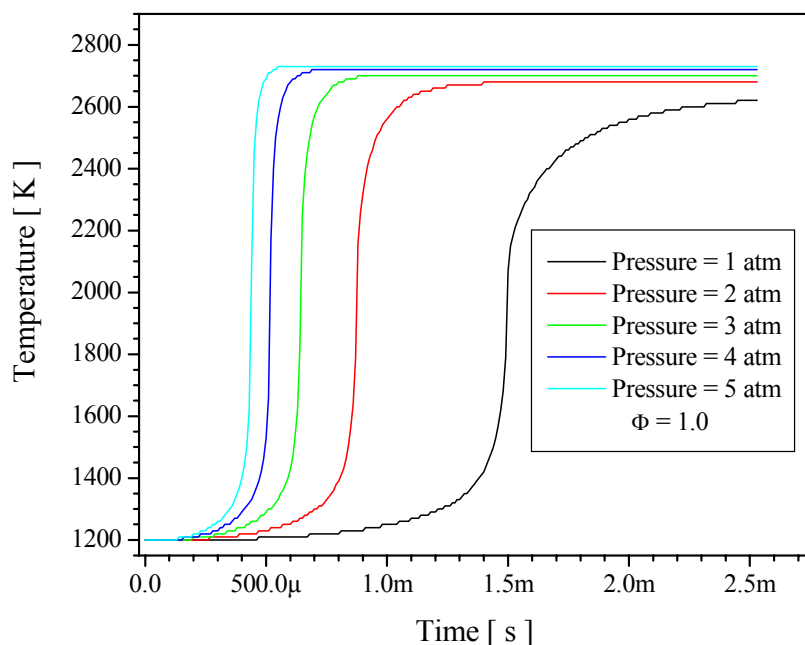
Figure 5. Time evolution of temperature as predicted by the Marinov mechanism for stoichiometric mixture and total pressure varying from 1 to 5 atm (obtained with CHEMKIN).
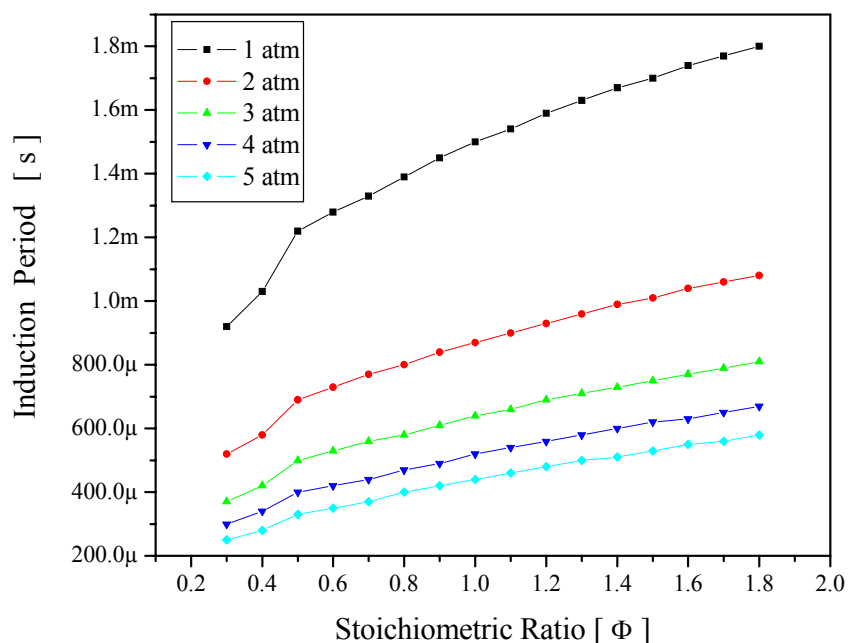

Figure 6. Variation of the induction period with the stoichiometric ratio for different values of pressure as predicted by the Marinov (1998) mechanism (obtained with CHEMKIN).

The smaller amount of *OH* in the final products for higher pressure may indicate a higher rate of radical recombination at higher pressure resulting in a larger conversion towards carbon dioxide and water. The hydroperoxy radical (HO_2) follows the same behavior as the hydroxyl radical. However, the formation and destruction of the methyl radical (CH_3) and of the carbon monoxide are strongly affected by the total system pressure. We also note a higher

conversion from carbon monoxide to carbon dioxide as the pressure increases. Both the carbon dioxide and the water present higher concentrations in the final products for higher system pressures.

Figure 8 shows the variation of the mole fractions of the main intermediate species and the saturated products as a function of the temperature during the transient variation of temperature, for the different pressures. We note that the effect of pressure occurs only at a limited range of the temperature evolution, especially for CO, H_2O and CO_2.
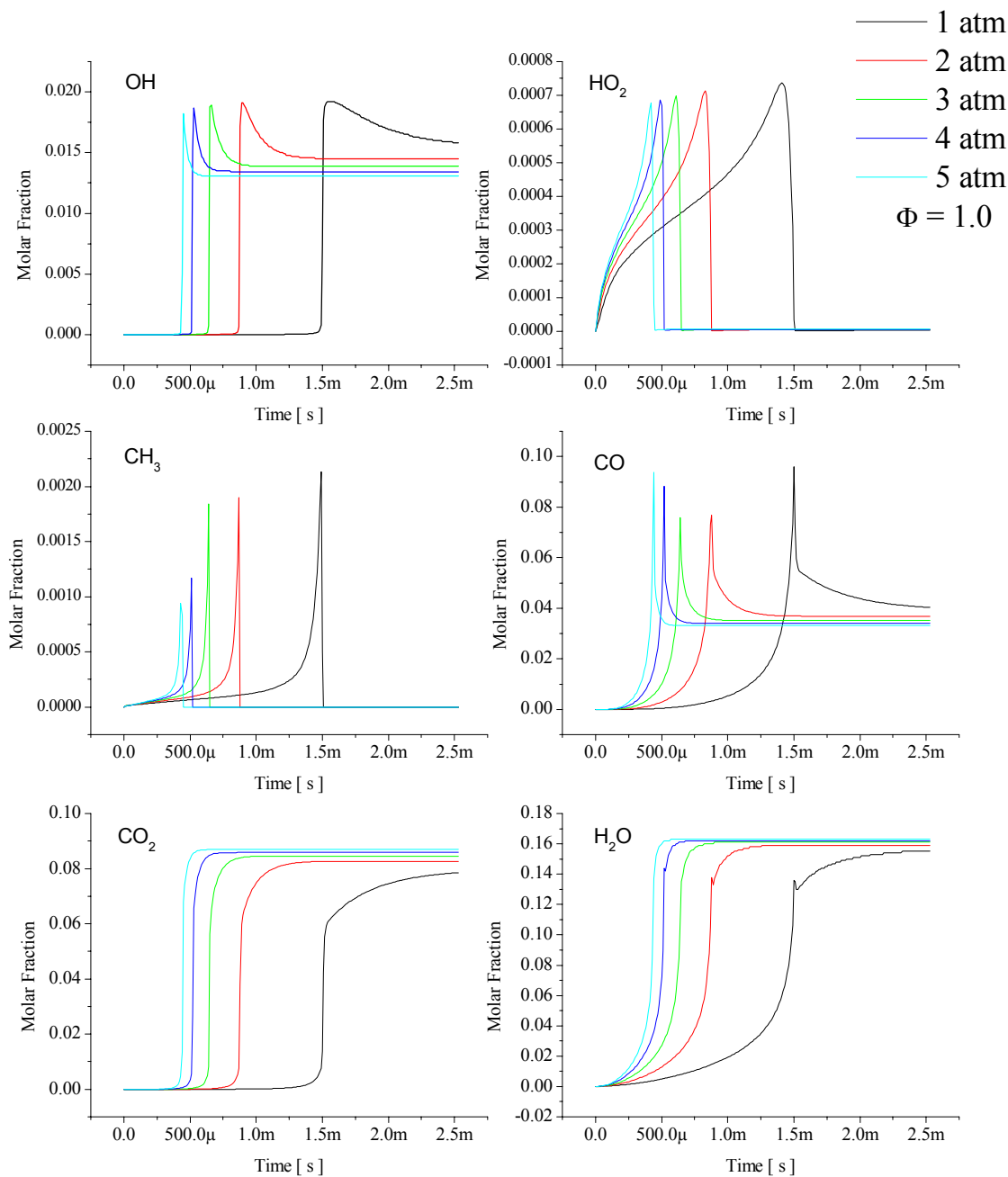

Figure 7. Time variation of the mole fractions of the major intermediate species (OH, CH_3, HO_2, CO) and the saturated combustion products (CO_2, H_2O) (obtained with CHEMKIN).
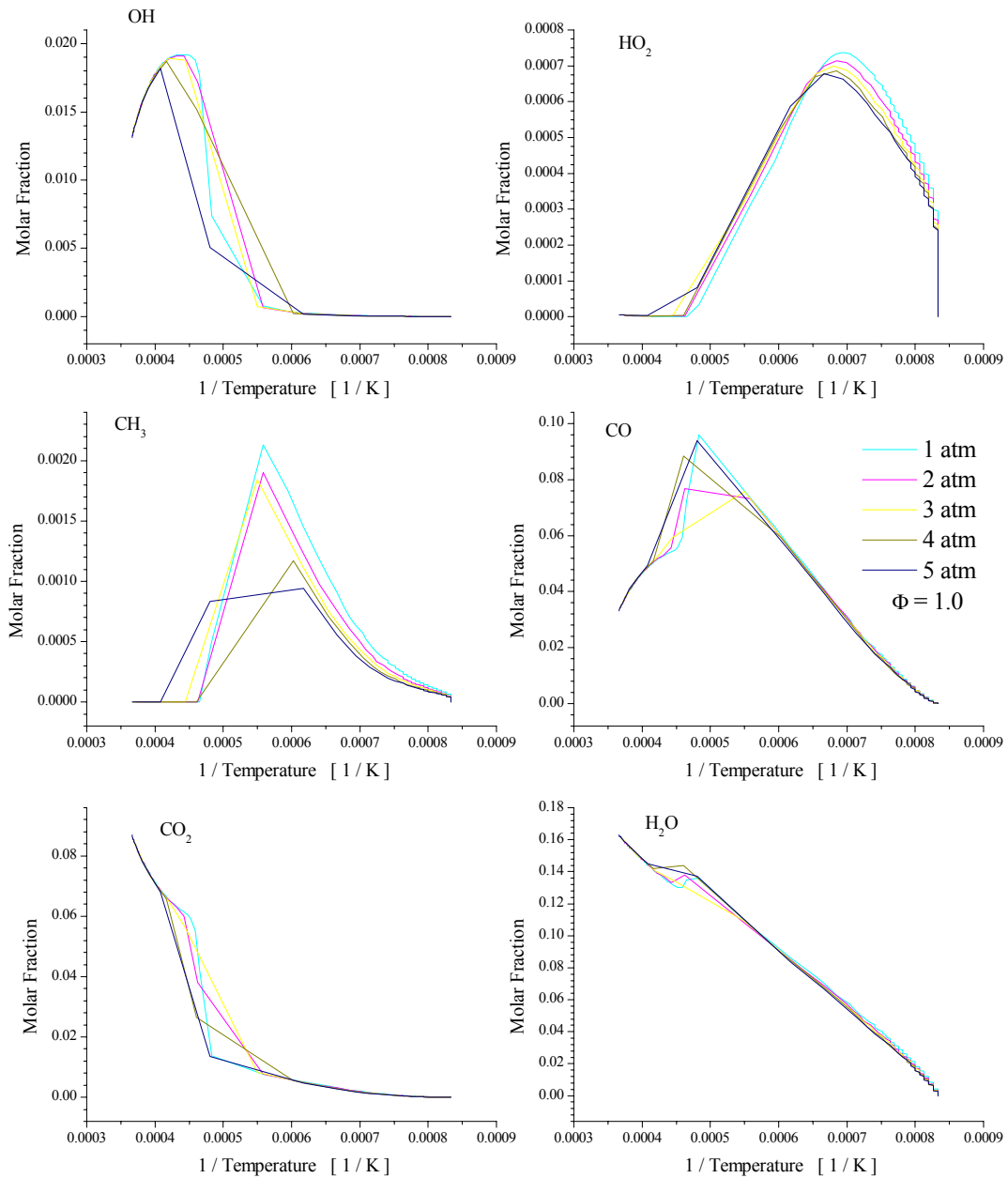
Figure 8. Variation of the mole fraction of the main intermediate species and of the saturated combustion products as a function of temperature for pressures varying from 1 to 5 atm (obtained with CHEMKIN).

4. Conclusion

Here, we analyzed numerically the thermal ignition of ethanol with dry standard air using two kinetic mechanisms available from the literature, the mechanisms by Marinov (1998) and by Konnov (2001). The softwares CANTERA (2001) and CHEMKIN (2003) were used to simulate the thermal ignition of ethanol in constant pressure, adiabatic, perfectly stirred reactor conditions. The induction period, the temperature and the time evolution of the mole fractions of intermediate species were observed as a function of pressure and stoichiometric ratio.

The main conclusions can be summarized as follows:

1. The results obtained from the Konnov (2000) mechanism show the same general trend when compared to the results from the Marinov (1998) mechanism, however, with a stronger dependency on the total pressure of the system. Both mechanisms result in the same final temperature for the same initial pressure. Therefore, while there is a consistency in the thermodynamic properties used, since the Marinov mechanism was extensively compared to measurements in the literature, we can conclude that the Konnov mechanism is not able to correctly predicting the rates of formation and destruction of intermediate species important in the decomposition of ethanol.

2. From the Marinov (1998) mechanism, the induction period increases as the initial mixture becomes lean in fuel, ranging from 1000 to 1800 μs at 1 atm and 200 to 500 μs at 5 atm. This behavior (not the values) is the same detected for the unsaturated aliphatic hydrocarbons

3. The time evolution of temperature becomes steeper and the induction period decreases with the increase in pressure. There is a small effect of the total pressure in the final temperature of the system. While the induction period decreases as the pressure is increased, it occurs at a smaller rate for the higher pressures. Although this general trend is also obtained from the Konnov mechanism, the absolute values of induction period are markedly different. The rate of change of the induction period with the stoichiometric ratio is approximately the same for pressures from 3 to 5 atm.

4. The variation in pressure does not have an important effect on the maximum amount of OH produced. The time variation of the mole fraction follows the same trends exhibited by the temperature, but the destruction of OH is progressively slower as the pressure is reduced. The smaller amount of OH in the final products for higher pressure may indicate a higher rate of radical recombination at higher pressure resulting in a larger conversion towards carbon dioxide and water. Therefore the dependency of induction time to stoichiometry reduces as the pressure is increased.

5. The hydroperoxy radical (HO_2) follows the same behavior as the hydroxyl radical. However, the formation and destruction of the methyl radical (CH_3) and of the carbon monoxide (CO) are strongly affected by the total system pressure. We also note a higher conversion from carbon monoxide to carbon dioxide as the pressure increases. Both the carbon dioxide and the water present higher concentrations in the final products for higher system pressures.

These conclusions are limited to the range of pressures for which the mechanisms, specially the Marinov mechanism, have been developed and validated. At the pressures typical of spark ignition internal combustion engines the results may vary, although it is not expected a complete change of the main conclusions. This work is being extended to relate the findings from chemical kinetics predictions to the conditions prevailing in spark ignition internal combustion engines. Also, the Konnov mechanism is being studied to correct the oxidation rates of ethanol in order to improve its overall prediction capability and allow its use as a general chemical kinetic mechanism for species up to C_3.

5. Acknowledgements

6. References

Cancino, L. R., 2004, "Análise de equilíbrio químico, cinética química da ignição térmica e propagação de chama plana laminar de misturas de hidrocarbonetos leves com ar". in Portuguese, M.Sc. Thesis, UFSC, 245 pp.

Cancino, L. R. and Oliveira, A. A. M., 2004, "Análise de equilibrio químico, cinética química da ignição térmica e propagação de chama plana laminar de misturas de hidrocarbonetos leves com ar". Proceedings of the ENCIT 2004, Rio de Janeiro, Oct. 2004, 11 pp.

Cancino, L. R. and Oliveira, A. A. M., 2005, "Influência da insaturação do carbono sobre o equilíbrio químico e ignição térmica de hidrocarbonetos alifáticos em ar". Proceedings of the X Latinamerican Congress of Heat and Mass Transfer. Caracas, Venezuela.

Cramer, C, J., 2002, "Essentials of Computational Chemistry, Theories and Models", John Wiley & Sons, USA.

Glassman, I. 1996. "Combustion" Third edition, Academic Press, USA.

Goodwin, D., "CANTERA Object-Oriented Sotfware for Reacting Flows", version 1.2, available in <www.cantera.org >.

Gordon Research Group, "GAMESS, General Atomic and Molecular Electronic Structure System", Iowa State University, USA. Disponivel em: <http://www.msg.ameslab.gov/GAMESS/GAMESS.html >

Kamalkumar I, *et al*, 2001, "Reaction kinetics measurements and analysis of reaction pathways for conversions of acetic acid, ethanol, and ethyl acetate over silica-supported Pt. Applied Catalysis A: General 222, 369-392.

Konnov, A., 2000, "Alexander Konnov´s Combustion Mechanism", available in <http://homepages.vub.ac.be/~akonnov/ >.

Konnov, A., 2005, "Personal Communication".

Kuo, K.,1986, "Principles of Combustion", JHON WILEY & SONS, USA

Marinov, N. M. 1998. "A detailed chemical kinetic model for high temperatura etanol oxidation". Lawrence Livermore Nartional Laboratory. USA.

Park, J., Zhu, R. S. and Lin, M. C., 2002, " Thermal decomposition of ethanol. I. ab initio molecular orbital/Rice-Ramsperger-Kassel-marcus prediction of rate constant and product branching ratios", Journal of Chemical Physics, V 117, Number 7.

Sandia National Laboratories, "CHEMKIN, Chemical kinetics" version 3.7.1, Reaction Desing, <www.reactiondesing.com >.

W. C. Gardiner, Jr. 2000. "Gas-Phase Combustion Chemistry". Springer-Verlag New York Inc. USA.

Warnatz, J., Maas, U. and Dibble, R. W., 1999, "Combustion, Physical and chemical fundamentals, Modeling and simulation, Experiments, Pollutant Formation." 2nd Edition. Springer, Germany.

7. Responsibility notice

The authors are the only responsible for the printed material included in this paper.